Investigating the synergistic potential Si and biochar to immobilize Ni in a Ni-contaminated calcareous soil after *Zea mays* L. cultivation

Hamid Reza Boostani[1], Ailsa G. Hardie[2], Mahdi Najafi-Ghiri[1], Ehsan Bijanzadeh[3], Dariush Khalili[4], Esmaeil Farrokhnejad[1]

[1]Department of Soil Science, College of agriculture and natural resources of Darab, Shiraz University, Darab74591, Iran.

[2]Department of Soil Science, Faculty of AgriSciences, Stellenbosch University, Private Bag X1, Matieland 7602, South Africa

[3]Department of agroecology, College of agriculture and natural resources of Darab, Shiraz University, Darab 74591, Iran

[4]Department of Chemistry, College of Sciences, Shiraz University, Shiraz 71454, Iran

Correspondence to: Hamid Reza Boostani (hr.boostani@shirazu.ac.ir)

Abstract. In Iran, a significant percentage of agricultural soils are contaminated with a range of potentially toxic elements (PTEs), including Ni, which need to be remediated to prevent their entry into the food chain. Silicon (Si) is a beneficial plant element that has been shown to mitigate the effects of PTEs on crops. Biochar is a soil amendment that sequesters soil carbon, and that can immobilize PTEs and enhance crop growth in soils. No previous studies have examined the potentially synergistic effect of Si and biochar on Ni concentration in soil chemical fractions and immobilization thereof. Therefore, the aim of this study was to examine the interactive effects of Si and biochar, to reduce Ni bioavailability and its corresponding uptake in corn (*Zea Mays*) in a calcareous soil. A 90-day factorial greenhouse study with corn was conducted. Si application levels were applied at 0 (S_0), 250 (S_1) and 500 (S_2) mg Si kg^{-1} soil and biochar treatments (3% wt.) including rice husk (RH) and sheep manure (SM) biochars produced at 300°C and 500°C (SM300, SM500, RH300 and RH500). At harvest, Ni concentration in corn shoots, Ni content in soil chemical fractions and release kinetic of DPTA-extractable Ni were determined. Simultaneous utilization of Si and SM biochars led to a synergistic reduction (15-36%) of Ni content in the soluble and exchangeable fractions compared to application of Si (5-9%) and SM (5-7%) biochars separately. The application of the Si and biochars also decreased DPTA-extractable Ni and Ni content in corn shoots (by up to 57%), with the combined application of SM500+S_2 being the most effective. These effects were attributed to the transfer of Ni in soil from more bioavailable fractions to more stable iron oxide bound fractions, related to soil pH increase. The SM500 was likely the most effective biochar due to its higher alkalinity and lower acidic functional group content which enhanced Ni sorption reactions with Si. The study demonstrates the synergistic potential of Si and sheep manure biochar at immobilizing Ni in contaminated calcareous soils.

1 Introduction

One of the most important ways for potentially toxic elements (PTEs) to enter the human food chain is through the consumption of plants grown in soils contaminated with PTEs. Potentially toxic elements pollute soil environments as a result of mining, metal smelting, use of sewage sludge and domestic and industrial effluents in agriculture especially in developing countries (Liu et al., 2018). Potentially toxic elements in soils cannot undergo biodegradation by

43 living organisms, so they possess great stability and longevity in the soil (Poznanović Spahić et
44 al., 2019). Unlike other PTEs found in soils, such as mercury (Hg), cadmium (Cd) and lead (Pb),
45 nickel (Ni) is essential for plant growth at very low concentrations. Nevertheless, at elevated
46 contents (>35 mg Ni kg^{-1} soil), Ni causes many physiological and morphological malfunctions in
47 plants and severely stunts their growth (Shahzad et al., 2018; Antoniadis et al., 2017). In a study
48 conducted by Shahbazi et al. (2022), the Ni weighted average concentration of the cultivated lands
49 of Iran in the vicinity of the industrial areas was reported 350 mg kg^{-1} soil. In these soils, the
50 pollution index (the ratio of the element concentration to the standard concentration) calculated
51 for the Ni is greater than 5, which indicates a severe degree of pollution from the point of view of
52 environmental protection. Shahbazi et al. (2020) collected 711 agricultural soil samples located at
53 different climate zones (extra arid, arid, semi-arid, Mediterranean, semi humid, humid and per-
54 humid based on the de Martonne classification system) of Iran and reported that the Ni content in
55 the soils was between 2.79 mg kg^{-1} and 770 mg kg^{-1} with an average of 68 mg kg^{-1} soil. The results
56 showed that the concentration of Ni in 11.3% of these soils was higher than the threshold value.
57 Removing PTEs from contaminated sites via traditional methods such as pump and treat
58 technologies, soil washing and excavation is very expensive and time-consuming, therefore, for
59 plant cultivation in these areas, low-cost and effective methods should be sought to stabilize PTEs
60 in soils and prevent them from being transferred to the plant (Gao et al., 2023).

61 Silicon (Si) is a valuable nutrient for plant growth, and it is only considered essential for
62 some plant species such as rice. Applying Si to the soil can enhance plant resistance against
63 biological and non-biological tensions, including physiological stress caused by PTEs in soil (Bhat
64 et al., 2019; Yan et al., 2018). The use of Si to promote plant growth and mitigate the toxicity of
65 PTEs is becoming increasingly popular in agriculture (Li, 2019; Adrees et al., 2015). The
66 application of Si in soils contaminated with PTEs may reduce the bioavailability of PTEs by
67 increasing soil pH, increasing the secretion of organic ligands by the roots and the formation of
68 insoluble compounds with PTEs, and ultimately enhancing plant growth (Bhat et al., 2019; Xiao
69 et al., 2021). The soil pH increase associated with Si application is attributed to the hydrolysis
70 reaction of the silicate anion in soil solution which generates hydroxyl ions (Ma et al. 2021).

71 Biochar can be used for a number of applications including as a soil amendment that
72 sequesters soil carbon (C) and for stabilization of PTEs in polluted sites (El-Naggar et al., 2018).
73 Biochar is a carbon-rich, porous organic material which is prepared in a limited or no oxygen
74 conditions by pyrolysis of organic wastes, including crop and animal residues, urban waste, wood
75 byproduct (Vickers, 2017; Ankita Rao et al., 2023). The organic surface functional groups of
76 biochar such as carboxylic and phenolic groups provide cation exchange capacity in soils
77 (Tomczyk et al., 2020). Addition of biochar to the soil not only improves the soil chemical and
78 physical properties, but also reduces the bioavailability of PTEs in contaminated soils through
79 some physicochemical processes such as sedimentation, complexation, and electrostatic
80 adsorption (Bandara et al., 2020; Deng et al., 2019; Derakhshan Nejad et al., 2018). The
81 complexation of Ni with oxygen-containing functional groups on biochar surfaces including
82 carboxyl, ether, carbonyl, and hydroxyl, has been identified as a key mechanism for Ni
83 immobilization in soil (Alam et al., 2018; El-Naggar et al., 2018). Electrostatic attraction of Ni by
84 negatively charged functional groups on the surfaces of biochar is another potential mechanism
85 for Ni stabilization in soil (Ahmad et al., 2014). Increased soil pH following the application of
86 biochar also promotes Ni adsorption reactions (Uchimiya et al., 2010). However, the efficiency of

biochar prepared from different feedstocks and under different production conditions in stabilizing PTEs in soils can vary significantly (Dey et al., 2023).

Potentially toxic elements in soil can exist in different chemical fractions such as water soluble and exchangeable (WsEx), bound to carbonates (Car), organic matter (OM), iron and manganese oxides (FeMnOx) and residual (Res) (found in minerals) (Singh et al., 1988). The bioavailability of these forms differs, the WsEx fraction has the highest bioavailability and the Res form is considered unusable by plants. PTEs in other chemical fractions in soils could be potentially accessible for plant roots depending on soil characteristics such as soil texture, soil pH and soil organic matter content (Kamali et al., 2011; Bharti et al., 2018). The diethylene triamine penta-acetic acid (DTPA) extraction is commonly employed for assessing Ni availability in calcareous soils (Lindsay and Norvell, 1978). However, it is important to acknowledge that this methodology solely assesses Ni availability for plants, while the quantity of released Ni may vary across distinct stages of plant development. Consequently, the examination of alterations in extractable Ni levels over time using the DTPA solution can prove valuable in estimating bioavailability of Ni in soil. The PTEs desorption capacities of soils are anticipated to be contingent upon factors such as soil pH, cation exchange capacity, the specific nature of metal ions, and the source of the metals (Kandpal et al., 2005). Furthermore, the release kinetic parameters can provide insight into the bonding mechanisms of PTEs in soils and their potential risk for leaching into groundwater or surface water (El-Naggar et al., 2021). Therefore, sequential extraction methods and release kinetic models have been employed to assess the efficacy of amendment materials in stabilizing PTEs in contaminated soils. Xiao et al. (2021) found that addition of mineral Si fertilizer to a contaminated paddy soil caused a significant decrease in the Cd and Pb fractions bound to carbonates and iron-manganese oxides while the residual and organic matter-bound forms experienced a notable increase. In another study, application of cotton residue biochar (1.5 wt. %) to a calcareous soil with a sandy loam textural class containing different levels of Cd contamination was more efficacious than corn and wheat straw biochars in decreasing Cd content in the WsEx and Car fractions and enhancing Cd concentration in the Res fraction. In addition, application of cotton residue biochar decreased EDTA-extractable Cd by 45–52% compared to the control (Boostani et al., 2023b).

As both biochars and Si are economical and effective soil amendments to reduce plant uptake of PTEs and stress in contaminated soils, their potential synergistic effect on the immobilization of PTEs in soils should be further investigated. Currently, no previous studies have examined the combined application effects of Si and biochars on the Ni content in various soil chemical fractions and release kinetic of Ni in calcareous soils. The primary objective of the present study was to elucidate the interaction of biochars and Si levels, to reduce bioavailability of Ni in soil and its corresponding accumulation in corn (*Zea Mays* L. 604) plant. Additionally, the study sought to elucidate the underlying soil chemical mechanisms that are likely to be responsible for such effects.

2 Materials and methods

2.1 Soil sampling, characterization and Ni treatment

A composite soil sample from the surface layer (0-30 cm) was collected with an auger at the research farm of the College of Agriculture and Natural Resources in Darab, southern Iran (28° 45′ 0.99″ N 54° 26′ 52.14″ E, Elevation 1105 m) (Fig. 1). The climate, mean annual precipitation, soil moisture and thermal regimes of the studied area were semi-arid, 250 mm, ustic

and hyperthermic respectively. The composite soil sample was placed in polyethylene bags in the field and then transported to laboratory where it was immediately air-dried, passed through a 2 mm sieve and then stored at room temperature until the physicochemical analysis was performed. Soil sand, silt and clay content were determined by the hydrometer method (Gee and Bauder, 1986). Soil pH and EC were determined using a saturated paste (Rhoades, 1996), while organic matter was determined using Walkley-Black procedure (Nelson and Sommers, 1996). Calcium carbonate equivalent (CCE) was determined by acid neutralization (Loeppert and Suarez, 1996), while cation exchange capacity was determined using 1M ammonium acetate (Merck, 99%) method (Sumner and Miller, 1996). Available Ni was determined using DPTA (Merck, 99%) extraction (Lindsay and Norvell, 1978). Plastic containers were filled with two kilograms of soil and then 500 ml $NiCl_2$ (Merck, 99%) solution was mixed into to them to achieve a Ni concentration of 300 mg Ni kg^{-1} soil. The Ni-treated soil samples were then allowed to dry out at room temperature, and then rewetted to field capacity using deionized water and allowed to dry out again. The rewetting and room temperature drying cycle was repeated three times to allow the Ni to equilibrate with the soil. The repeated wetting and drying cycles were performed to simulate field processes (Boostani et al., 2023c). The incubation period was 60 days and the ambient temperature was 25±2 ºC.
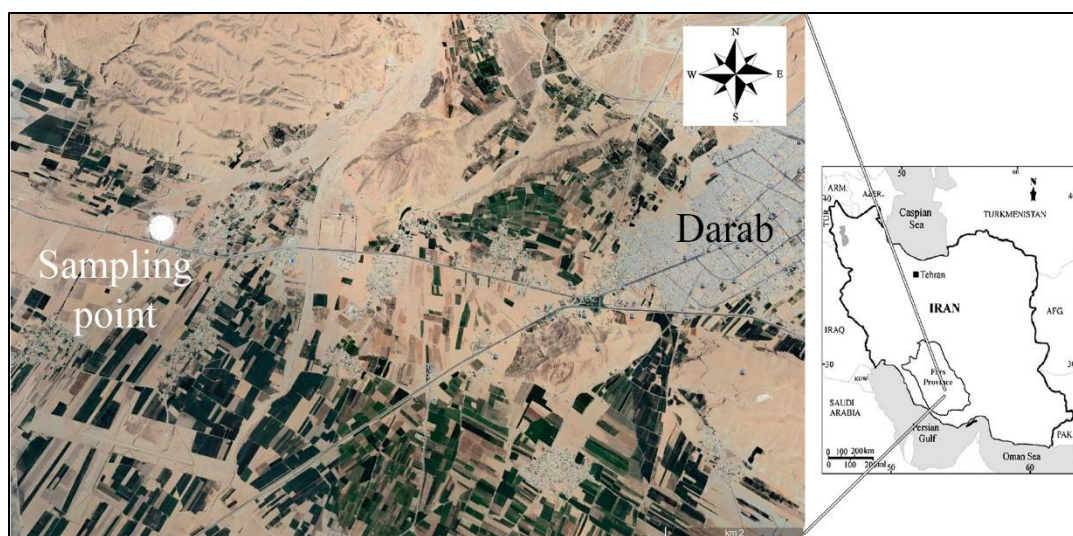
Fig. 1. The location of soil sampling in Darab region, southern Iran.

2.2 Production of biochar and its properties

The sheep manure and rice husk were respectively procured from an active animal husbandry and rice mill factory situated in the Darab region, Fars province, Iran. Subsequently, the raw materials underwent a 1-week period of air-drying, followed by electrical milling and sieving through a 2 mm mesh. A slow pyrolysis procedure (2 h at 300 °C and 500 °C) in an oxygen-limited environment was carried out to generate biochars from feedstocks (Anand et al., 2023). The generated biochars were then cooled at ambient temperature and sieved with a 0.5 mm mesh to ensure consistent particle size. The chemical characteristics of the biochars were assessed using

the following standard methods. Biochar pH and EC were determined in a 1:10 deionized water suspension (Sun et al., 2014), while CEC was determined using the method of Abdelhafez et al. (2014). Biochar total C, N and H contents were determined by elemental analyzer (ThermoFinnigan Flash EA 1112 Series, Thermoscientific, USA). Biochar moisture and ash content were determined by heating in an oven, while the O+S content was calculated by subtraction of C, N, H, ash and moisture content from total biochar mass (Keiluweit et al., 2010). Biochar total Ni content was determined by combustion and dissolution of the ash in 2M HCl (Merck, 37%) (Boostani et al., 2018b). The Ni content in the acid solution was determined using atomic absorption spectroscopy (AAS) (PG 990, PG Instruments Ltd., UK). Surface functional groups of the biochars were assessed using Fourier Transform Infrared (FTIR) spectroscopy using a Shimadzu DR-8001 instrument and KBr pellet transmission method. The morphology of surface biochar was assessed using scanning electron microscopy (SEM) (TESCAN-Vega3, Czech Republic).

2.3 Greenhouse experiment

A completely randomized factorial experiment was conducted in a greenhouse environment with three replications. The first factor consisted of the biochar treatments including rice husk (RH) and sheep manure (SM) generated at 300 °C and 500 °C (Control (C) (with no biochar), SM300, SM500, RH300 and RH500), each at the level of 3%wt. The second factor included Si application levels (0 (S_0), 250 (S_1) and 500 (S_2) mg Si kg^{-1} soil) supplied as Na_2SiO_3 (Sigma Aldrich, 98%) solution. Based on the experimental design, Si levels were added to the 2 kg of Ni-treated soil samples and after drying the soil and mixing it, the prepared biochars were added to the required amount. Immediately after that, the treated soil samples were transferred to plastic pots (45 pieces each containing 2 kg soil) and to facilitate the required reactions, the moisture content of the samples was kept at field capacity level for a duration of two weeks. Thereafter, 6 corn seeds (*Zea mays* L. 604) were planted in each pot, and at the 4-leaf stage, 2 plants were kept in each pot until the end of cultivation. During the growth of the plant, distilled water was used to maintain the soil moisture content in the pots at field capacity. After 90 days, the plants were harvested at the soil interface, rinsed with distilled water to remove contamination, immediately air-dried and kept for Ni determination of plant shoots. After separating the roots, the soil from the pots was immediately air-dried, and then passed through a 2 mm sieve and stored in labelled polyethylene bags at room temperature, to be subsequently utilized for performing Ni sequential extraction and release kinetics.

2.4 Sequential extraction procedure

The present study employed a successive extraction technique (Singh et al., 1988) to fractionate Ni in the following soil chemical fractions, namely water-soluble and exchangeable (WsEx), carbonate-bound (Car), organic matter-bound (OM), manganese oxide-bound (MnOx), amorphous iron oxide-bound (AFeOx), crystalline iron oxide-bound (CFeOx), and residual (Res). The methodological specifics are provided in Table 1.

Table 1
Successive extraction technique of Singh et al. (1988)

Chemical speciation containing Ni	acronym	Duration of agitation (h)	Extractants	Relative density (g.cm^{-3})
Exchangeable and soluble	WsEx	2.0	1 M magnesium nitrate (Merck, 98%)	1.10
Carbonate	Car	5.0	1 M sodium acetate (Merck, 99%) (pH=5)	1.04
Organic	OM	0.5	0.7 M sodium hypocholoride (pH=8.5)	1.00
Mn oxide	MnOx	0.5	0.1 M hydroxyl amine hydrochloride (Merck, 98%) (pH=2 by nitric acid (Merck, 65%))	1.00
Amorphous Fe oxides	AFeOx	0.5	0.25 M hydroxyl amine hydrochloride (Merck, 98%) + 0.25 M choloridric acid (Merck, 37%)	1.01
Crystalline Fe oxides	CFeOx	0.5	0.2 M ammonium oxalate (Merck, 99%) + 0.2 M oxalic acid (Merck, 99%) + 0.1 M ascorbic acid (Merck, 99.7%)	1.02

201

202 2.5 Release kinetics experiment

203 A 50 ml centrifuge tube was filled with 10 g of soil. After that, 20 ml of DTPA solution
204 (0.005 M DTPA (Merck, 99%) + 0.1 M tri-ethanol amine (Merck, 99%) + 0.01 M calcium chloride
205 (Merck, 97%)) (pH: 7.3) (Lindsay and Norvell, 1978) was added to the soil. The soil-DTPA
206 mixtures were stirred for specific periods of time, i.e. 5, 15, 30, 60, 120, 360, 720 and 1440 minutes
207 at a constant temperature (25 $\pm$2 °C). After each stirring time, the soil suspension was centrifuged
208 (2683 $\times$ g) to separate the soil particles from the liquid phase. Atomic absorption spectroscopy
209 (AAS) (PG 990, PG Instruments Ltd., UK) was used to analyze the Ni concentration in the liquid
210 phase. The Ni concentration in the liquid phase versus time was plotted to obtain a Ni release
211 kinetic curve. A total of seven kinetic models namely order models (zero, first, second and third),
212 parabolic diffusion, power function and simple Elovich were assessed to fit the Ni release data.
213 The best models for describing the data were selected according to the maximum value of the
214 coefficient of determination (R^2) and the minimum amount of the standard error of estimate (SEE)
215 (Nasrabadi et al., 2022).

216 2.6 Data analysis

217 The ANOVA test was utilized to assess treatments effects between the individual and
218 combined biochar and silicon treatments. Additionally, a comparison of means was conducted
219 using the MSTATC computer program, applying Duncan's test with a significance level of 5%.
220 Figures were generated using Excel 2013 software. Pearson correlation coefficients among
221 parameters in the dataset were determined using SPSS 12.0.

222 **3 Results and Discussion**

223 3.1 Soil characteristics
224 The soil used in the study prior to experimental treatment, exhibited a sandy loam texture
225 and possessed alkaline properties with significant calcium carbonate content (calcareous soil),
226 while not being classified as saline (Table 2). The quantity of soil organic matter (OM) and cation
227 exchange capacity (CEC) were extremely low (Table 2) compared to the values (OM: 1.20-7.10%,
228 CEC: 19.5-55.9 cmol$_{(+)}$ kg^{-1}) documented by Rassaei et al. (2020) for calcareous soils of Fars
229 province, southern Iran. The soils in Iran mainly originate from calcareous alluvium under xeric,

230 ustic or aridic and mesic, thermic or hyperthermic moisture and temperature regimes, respectively.
231 These soils have varied properties such as calcium carbonate equivalent (1-81%), clay content (1-
232 75%), EC (0.40-49.0 dS m^{-1}), organic matter (0.10-21.5%) and gypsum content (0-91%) (Ghiri et
233 al., 2011). Furthermore, it should be noted that the concentration of available Ni extractable by
234 DTPA in the soil was low (Table 2) compared to the mean value (0.60 mg Ni kg^{-1}) reported by
235 Jalali et al. (2022) for calcareous soils located at western Iran.

236

Table 2
Certain physicochemical attributes of the soil prior to cultivation.

Sand (%)	58.0
Silt (%)	30.0
Clay (%)	12.0
Soil textural class	Sandy loam
pH$_{(s)}$	7.59
EC (dS m^{-1})	2.60
CCE (%)	55.0
OM (%)	0.50
CEC (cmol$_{(+)}$kg^{-1})	11.7
Total Ni (mg kg^{-1})	28.0
Ni-DTPA (mg kg^{-1})	0.39

Notes: EC, electrical conductivity; OM, organic matter; CCE, calcium carbonate equivalent; CEC, cation exchange capacity.

237

238 3.2 Chemical characteristics of the biochars

239 As the pyrolysis temperature rose from 300 °C to 500 °C, the SM biochars demonstrated
240 elevated pH and EC values, with the highest levels observed at the highest temperature (Table 3).
241 The elevated levels of alkali salts, which are reflected in the high ash content (Table 3), are the
242 contributing factor behind this observation in the SM biochars in comparison to the RH biochars.
243 Plant-based biochars commonly exhibit reduced levels of dissolved solids in comparison to
244 animal-based biochars (Sun et al., 2014). The SM300 biochar possessed the highest CEC value of
245 19.70 cmol$_{(+)}$ kg^{-1}. The observed phenomenon may be attributed to the diminution of surface
246 functional groups, namely carboxyl and phenol, at elevated pyrolysis temperatures. These groups
247 are predominantly responsible for facilitating the cation exchange capacity (CEC) of biochars
248 (Tomczyk et al., 2020). As the pyrolysis temperature increased, there was an observed increase in
249 the C content of the biochars, and a corresponding decrease in the content of hydrogen, oxygen,
250 and nitrogen (Table 3). The observed increase in the concentration of C as pyrolysis temperature
251 rises is consistent with a concomitant rise in the degree of carbonization. The observed reduction
252 in the levels of H and O might be attributed to the occurrence of dehydration reactions,
253 decomposition of oxygenated bonds, and the liberation of low molecular weight byproducts rich
254 in H and O, as recently noted by Zhao et al. (2017). Nitrogen compound volatilization explains the
255 diminished N content of the biochars at elevated pyrolysis temperatures. The ratios of H:C and
256 O:C are significant indicators of the aromaticity and polarity of biochars; the lower the ratios the
257 more condensed aromatic C the biochar contains (Chatterjee et al., 2020). The results shown in
258 Table 3 indicate that the H:C and O:C mole ratios showed a gradual decrease as the pyrolysis

temperature was increased, which can be interpreted as a sign of improved carbonization of the biochars (Zhao et al., 2017). The Ni content in the biochars derived from rice husk was below detection, whereas a limited quantity of Ni was detected in the biochars produced from sheep manure (Table 3).

Table 3
Some physical and chemical properties of the biochars.

	SM300	SM500	RH300	RH500
pH (1:20)	9.96	11.0	9.00	10.3
EC (1:20) (dS m^{-1})	3.94	4.28	0.84	1.17
CEC (cmol$_+$ kg^{-1})	19.7	18.9	18.9	15.3
C (%)	25.4	31.8	45.0	50.0
H (%)	1.85	0.80	2.28	1.06
N (%)	2.10	1.57	1.30	1.10
Ni (mg kg^{-1})	3.00	15.4	Nd	Nd
Moisture content (%)	1.91	1.82	2.65	2.37
Ash content (%)	53.8	60.0	34.2	44.8
H:C mole ratio	0.87	0.30	0.60	0.25
O+S:C mole ratio	0.44	0.09	0.24	0.01

Notes: SM300, sheep manure biochar generated at 300 °C; SM500, sheep manure biochar generated at 500 °C; RH300, rice husk biochar produced at 300 °C; RH500, rice husk biochar produced at 500 °C; CEC, cation exchange capacity; EC, electrical conductivity; Nd, non-detectable.

3.3 Biochar analysis using FTIR and SEM

The FTIR spectra of the SM and RH biochars are shown in Figure 2. The SM and RH biochars produced at 300 °C contained a higher content of carboxyl groups (1700 cm^{-1}) (Keiluweit et al., 2010) than the biochars produced at 500 °C, which is in agreement with the O:C values of the biochars (Table 3). All of the biochars contained absorption bands associated with lignin (1430 cm^{-1}) and cellulose (1030 - 1160 cm^{-1}) (Keiluweit et al., 2010). The SM biochar contained more calcite than the RH biochar as indicated by the greater intensity of calcite characteristic peaks at 1432, 875, and 711cm^{-1} (Myszka et al., 2019) in the SM biochars (Fig. 2a). There was also evidence of the presence of Ca oxalate in the SM biochars, indicated by the characteristic peaks at 1618, 780 and 518 cm^{-1} (Maruyama et al., 2023). All the biochars contained silica as indicated by the intense silica absorption peaks at 1100, 800 and 470 cm^{-1} (Zemnukhova et al., 2015).

277

278
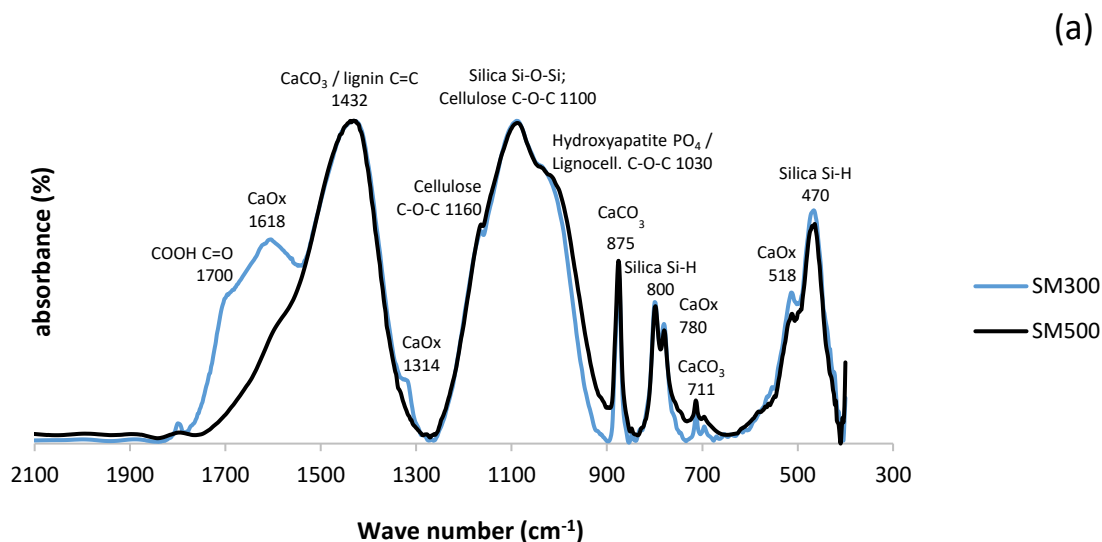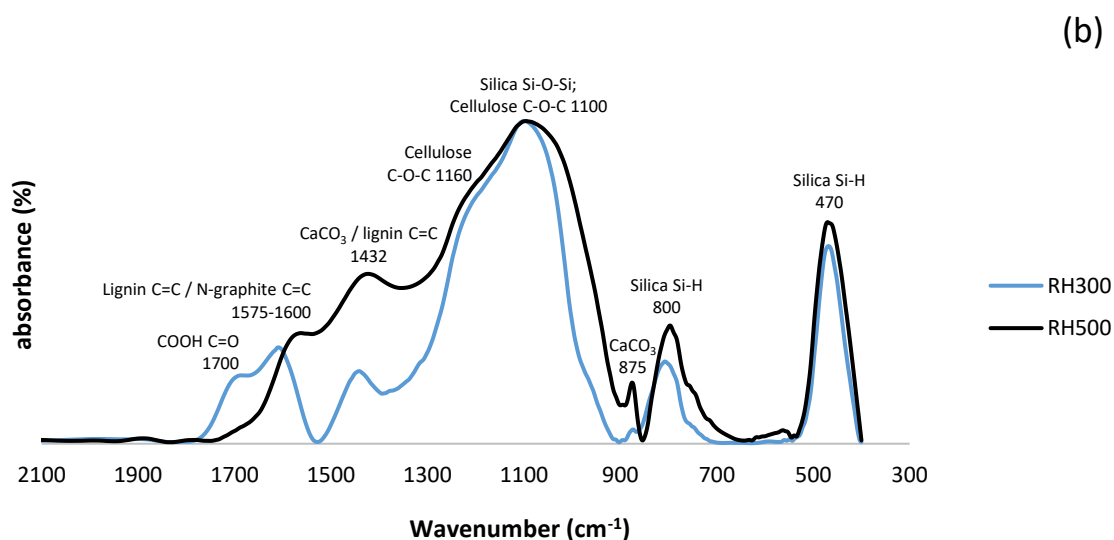
Fig. 2. FTIR spectra the biochars in the wave number range of 400-2000 cm^{-1}. Notes: SM300, sheep
manure biochar produced at 300 °C; SM500, sheep manure biochar produced at 500 °C; RH300, rice husk biochar
produced at 300 °C; RH500, rice husk biochar produced at 500 °C.

The SEM images of the SM and RH biochars are shown in Figure 3. The morphology of
the biochars became more rigid and porous at higher temperatures, as evidenced by the cell wall
shrinkage attributed to devolatilization of organic tissues (Claoston et al., 2014).

287
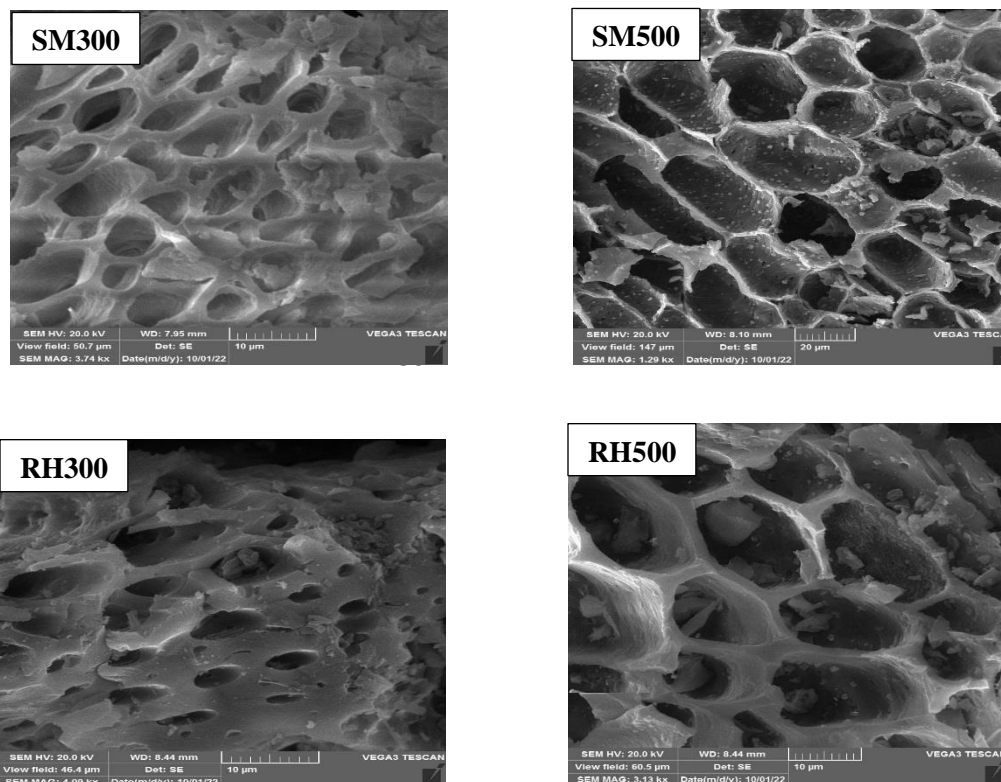
Fig. 3. SEM images of the biochars. Notes: SM300, sheep manure biochar produced at 300 °C; SM500, sheep manure biochar produced at 500 °C; RH300, rice husk biochar produced at 300 °C; RH500, rice husk biochar produced at 500 °C.

291

292   3.4 Nickel content in various soil chemical fractions after the application of Si levels and biochars

293   The interaction of treatments (biochars and Si levels) had a statistically significant effect
294   (P<0.01) on Ni concentration in all the soil chemical fractions, except for the Car fraction.
295   Whereas the main effects of individual treatments (biochars and Si levels) on Ni
296   concentration in all the soil chemical fractions were significant. The Ni concentration in
297   the WsEx fraction was significantly reduced by the application of Si levels (S_0 to S_2) from
298   6.07 mg Ni kg^{-1} to 5.17 mg Ni kg^{-1} by 14.8% (Table 4). Among the biochar treatments, the
299   greatest decrease in Ni content in the WsEx fraction compared to the control was due to
300   SM500 from 6.04 mg Ni kg^{-1} to 5.01 mg Ni kg^{-1} by 17%, while the RH300 treatment had
301   no significant effect (Table 4). The interaction effects of treatments indicated that the
302   lowest Ni content in the WsEx fraction was due to the combined treatment of SM500+S_2
303   (4.04 mg Ni kg^{-1} soil) (Table 4). The combined treatment of S_2 and SM biochars had strong
304   synergistic effect on reducing Ni content in the WsEx fraction (23-36% reduction)
305   compared to the sum of the treatments alone (13-15% reduction) (Fig. 4). Whereas this
306   synergistic effect of the combined treatments was not evident for the RH biochars (Fig. 4).
307   There was a negative correlation between Ni content in the WsEx fraction and soil pH ($r =$
308      $-0.66, p < 0.01$) indicating that the reduction in Ni content in the WsEx fraction was
309   strongly linked to the increase in soil pH due to the amendments (Supplementary
310   information). Previous studies have also shown that application of biochars and silicates

311 result in increases in soil pH, thus reducing the bioavailability of PTEs and their
312 conveyance to plant roots (Shen et al., 2020; Ma et al., 2021). Among the applied biochars,
313 the maximum pH and ash content (Table 3) and calcite (lime) content (Fig. 2) were
314 attributed to the SM500 biochar. Therefore, the combined $SM500+S_2$ was most effective
315 at reducing Ni content in the WsEx fraction, likely due to the higher alkalinity and ash
316 content of SM500 promoting Ni precipitation and adsorption (Sachdeva et al., 2023). The
317 increase in soil pH due to Na metasilicate also likely enhanced the precipitation of Ni in
318 the forms of Ni silicate and hydroxide. Addition of Si in the form of Na metasilicate
319 increases soil pH due to the hydrolysis of the silicate anion in soil solution which generates
320 hydroxyl ions (Ma et al., 2021).

321
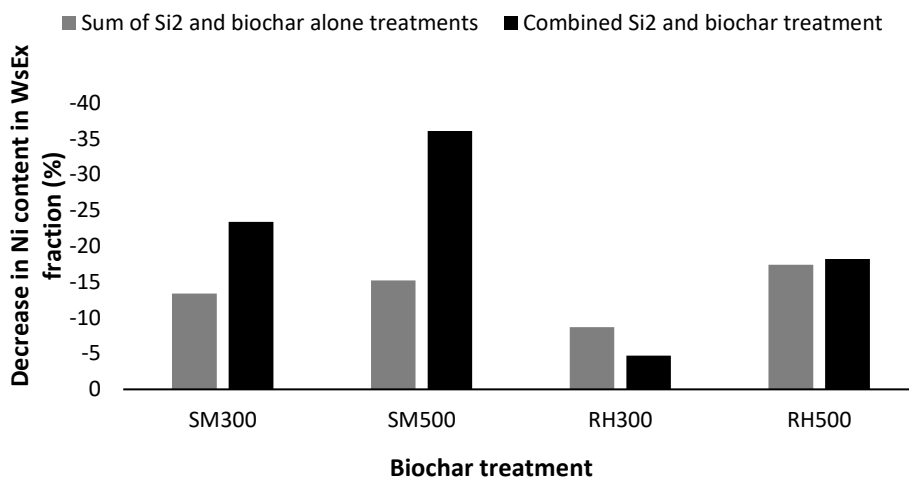
Fig. 4. Comparison of the effect of sum of the Si_2 and biochar alone treatment versus the combined
Si_2 and biochar treatments on the reduction of Ni content in the WsEx fraction. Notes: SM300, sheep
manure biochar produced at 300 °C; SM500, sheep manure biochar produced at 500 °C; RH300, rice husk biochar
produced at 300 °C; RH500, rice husk biochar produced at 500 °C.

326 The reduced effectiveness of biochars produced at 300 °C, as compared to those produced
327 at 500 °C, in decreasing Ni content in the WsEx fraction could also be attributed to the lower rates
328 of microbial oxidation and mineralization of RH500 and SM500, which is reflected in their greater
329 environmental stability (as indicated by the lower H/C mole ratio values) (Table 3). Consequently,
330 biochar produced at 500 °C may not provide sufficient acidic carboxyl functional groups to the
331 soil to stimulate SOM decomposition, leading to a greater increase in soil pH (Sun et al., 2023).
332 According to Zhu et al. (2015), the addition of wine lees-based biochar (a material from a wine
333 processing factory) to a heavy metal-contaminated soil (at levels of 0.5% and 1% w/w) resulted in
334 an increase in soil pH and a decrease in Ni content in the WsEx fraction.

335

336

337

338

Table 4

Effects of biochars and Si application levels on the Ni concentration (mg kg^{-1}) in different soil chemical fractions after corn cultivation.

	C	SM300	SM500	RH300	RH500	Mean
			WsEx			
S_0	6.32 a	6.02 a-c	5.91 bc	6.31 a	5.77 c	**6.07 A**
S_1	6.03 a-c	5.37 d	5.09 de	6.25 ab	5.28 d	**5.60 B**
S_2	5.77 c	4.84 e	4.04 f	6.02 a-c	5.17 de	**5.17 C**
Mean	**6.04 A**	**5.41 B**	**5.01 C**	**6.20 A**	**5.41 B**	
			OM			
S_0	9.72 a	10.6 a	8.04 d-f	10.0 a	9.02 b	**9.40 A**
S_1	9.60 a	9.75 a	7.16 g	8.62 b-d	8.70 bc	**8.76 B**
S_2	8.11 c-f	7.94 ef	7.12 g	8.30 c-e	7.63 fg	**7.82 C**
Mean	**9.14 A**	**9.28 A**	**7.44 C**	**8.99 A**	**8.44 B**	
			MnOx			
S_0	11.6 a	3.77 kl	5.99 f	4.69gh	9.71 c	**7.15 A**
S_1	10.3 b	3.50 l	5.00 g	4.57 hi	8.93 d	**6.48 B**
S_2	10.3 b	2.98 m	4.28 ij	3.96 jk	7.94 e	**5.89 C**
Mean	**10.7 A**	**3.42 E**	**5.09 C**	**4.41 D**	**8.86 B**	
			AFeOx			
S_0	11.1 ef	10.4 g	11.8 d	11.0 fg	11.7 de	**11.2 C**
S_1	12.2 b-d	10.7 fg	12.0 cd	12.2 b-d	12.7 bc	**12.0 B**
S_2	12.8 b	12.2 b-d	12.2 b-d	12.3 b-d	14.2 a	**12.7 A**
Mean	**12.1 B**	**11.1 C**	**12.0 B**	**11.8 B**	**12.9 A**	
			CfeOx			
S_0	77.3 f	78.0 f	84.0 cd	84.7 cd	79.6 ef	**80.7 C**
S_1	77.9 f	82.2 de	86.3 bc	85.1 b-d	83.6 cd	**83.0 B**
S_2	79.9 ef	85.5 bc	87.9 ab	85.7 bc	90.4 a	**85.9 A**
Mean	**78.4 C**	**81.9 B**	**86.0 A**	**85.2 A**	**84.5 A**	
			Res			
S_0	200 c-e	207 a	200 c-e	196 f	198 d-f	**200 A**
S_1	200 c-e	204 b	200 c-e	197 ef	195 f	**199 A**
S_2	200 cd	204 b	201 c	199 c-e	190 g	**199 A**
Mean	**200 B**	**205 A**	**200 B**	**198 B**	**195 BC**	

Notes: C, control; SM300, sheep manure biochar produced at 300 °C; SM500, sheep manure biochar produced at 500 °C; RH300, rice husk biochar produced at 300 °C; RH500, rice husk biochar produced at 500 °C; S_0, without Si addition; S_1, application of 250 mg Si kg^{-1} soil; S_2, application of 500 mg Si kg^{-1} soil. WsEx, water soluble and exchangeable fraction; OM, organic fraction; MnOx, bound to manganese oxides; AfeOx, bound to amorphous iron oxides; CfeOx, bound to crystalline iron oxides; Res, residual fraction; MF, mobility factor.

*Numbers followed by same letters in each column and rows, in each section, are not significantly (P<0.05) different

As there was no significant interaction effect between biochar type and Si levels on the Ni concentration in the Car fraction, only the significant individual main effects of biochar and Si levels are shown in Fig. 5. Changing the Si application levels from S_0 to S_2 significantly decreased the Ni content in the Car fraction by 11.7% (from 15.2 mg Ni kg^{-1} soil to 13.5 mg Ni kg^{-1} soil) (Fig. 5). The decrease in the concentration of Ni in the Car form with an increase in the Si levels could potentially be explained by the competition between silicate (SiO$_4^{-4}$) and carbonate ions for binding with Ni^{2+} ions in the soil solution (Sparks et al., 2022). The SM biochars had no significant effect on the Ni concentration in the Car fraction whereas addition of RH biochars led to a significant increase in the Ni concentration in this fraction (Fig. 5). Ippolito et al. (2017) found

that addition of two biochars (pine [*Pinus contorta*] and tamarisk [*Tamarix* spp.]) to a soil contaminated by mining activities caused a significant increase in the soil Cd content bound to carbonates. They concluded that the reduction in Cd bioavailability may have been due to the ability of biochar to raise soil pH levels and induce the precipitation of $CdCO_3$. Similarly, Yuan et al. (2011) proposed that the decrease in bioavailability of PTEs in soil amended by biochars derived from different crop residues might have been caused by the creation of metal-carbonate species and carbonate-surface functional group reactions, which could function as a mechanism for sequestration.
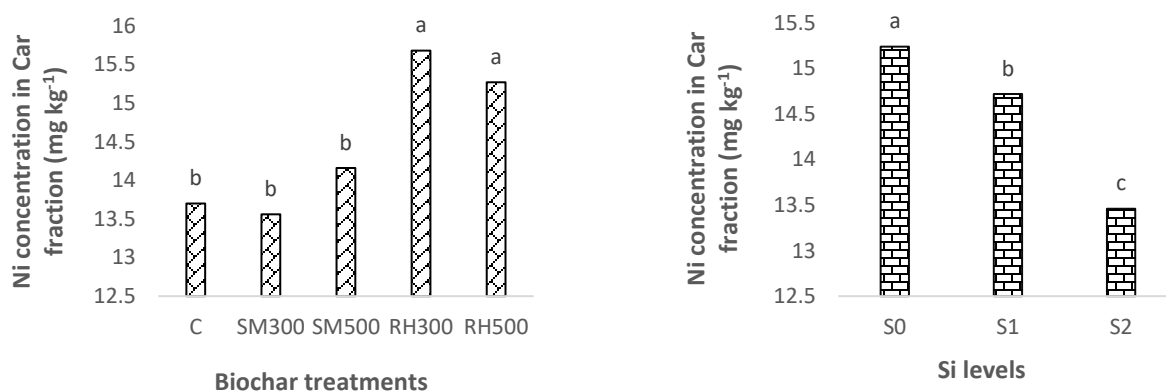
Fig. 5. Main effects of (a) biochar type and (b) Si application levels on the Ni concentration (mg kg^{-1}) in the Car fraction after corn cultivation. Notes: C, control; SM300, sheep manure biochar produced at 300 °C; SM500, sheep manure biochar produced at 500 °C; RH300, rice husk biochar produced at 300 °C; RH500, rice husk biochar produced at 500 °C; S_0, without Si addition; S_1, application of 250 mg Si kg^{-1} soil; S_2, application of 500 mg Si kg^{-1} soil. * Numbers followed by same letters in each section, are not significantly (P<0.05) different.

The biochars produced at 300 °C had no significant effect on the Ni content in the OM fraction compared to control, while the biochars generated at 500 °C significantly decreased it (Table 4). The greatest reduction in Ni content in the OM fraction (18.6%) was found to be in that which underwent the SM500 treatment. Lu et al. (2017) explored how the application of bamboo and rice straw biochars with varying mesh sizes (0.25 and 1 mm) and at three different levels (0, 1, and 5% w/w) affected the distribution of Cd in a contaminated sandy loam soil, using the BCR **(**Bureau Communautaire de Référence) sequential extraction method. In contrast to the present study, they reported that the biochars increased the concentration of Cd in the OM fraction, and this was closely related to the increase in Cd immobilization. In another study, the application of sheep manure biochar produced at 500 °C at the rate of 3% wt. to a Cd-contaminated calcareous soil resulted in a significant increase in Cd content in the OM fraction, whereas the addition of other biochar treatments (wheat straw, corn straw, rice husk, licorice root pulp) caused a significant decrease in the concentration of Cd in the OM fraction when compared to the control soil (Boostani et al., 2018a). In the study conducted by Boostani et al. (2018), the reduction in Cd concentration in the OM fraction as affected by application of rice husk biochar is in line with our results,

however; the increase in Cd content in the OM form with addition of sheep manure biochar is in contrast with the result of the present study. These observations indicate that in addition to the characteristics of biochar and the level of its application (Lu et al., 2017), soil characteristics (calcium carbonate percentage, soil texture, etc.) and the type of heavy metal can also have a substantial role in the binding of PTEs to soil organic matter. Changing the Si levels from S_0 to S_2 reduced the Ni concentration in the OM fraction by 16.8% (Table 4). Ma et al. (2021) reported that the application of Si to cultivated soils significantly reduced soil organic matter content, which could explain why the Ni concentration in OM fraction was reduced in the present study. They indicated that Si facilitates the decomposition of organic matter by enhancing soil pH. In this study, the interaction effects of biochars and Si levels showed that the lowest Ni content in the OM fraction was due to the combined treatment of SM500+S_2 (7.12 mg Ni kg^{-1} soil), which was equal to a 26.7% decrease compared to the control (CS$_0$) (9.72 mg Ni kg^{-1} soil) (Table 4).

All the biochar treatments caused a significant decrease in Ni content in the MnOx fraction compared to the control, with the greatest reduction caused by the SM300 treatment at 52.6% (Table 4). The lower temperature biochars were more effective than the higher temperature biochars in decreasing the Ni content in the MnOx fraction (Table 4). In agreement with the present study, Boostani et al. (2023c) observed that biochars produced from cow manure, municipal solid waste and licorice root pulp at a lower pyrolysis temperature (300 °C) decreased the Ni content in the MnOx fraction to a greater extent than those prepared at a higher temperature (600 °C). Hydrophobicity of biochar is decreased with increasing pyrolysis temperature (Kameyama et al., 2019). It is well known that, at the same soil water content, the water content of soil pores treated with biochars produced at lower pyrolysis temperatures is higher due to lower absorption of water by the biochars. Therefore, in soils with high soil pore water content and low oxygen conditions, the concentration of MnOx is decreased due to chemical reduction, while concomitantly, the Mn concentration in the exchangeable and water-soluble are increased (Sparrow and Uren, 2014). Furthermore, increasing the Si application levels from S_0 to S_2 significantly decreased the Ni content in the MnOx fraction by 17.6% (Table 4). Compared to the control, which had the highest concentration of Ni in the MnOx fraction (11.58 mg Ni kg^{-1} soil), the greatest interactive effect in the reduction of this fraction was related to the combined SM300+S_2 (2.98 mg Ni kg^{-1} soil) treatment by 3.8-fold (Table 4). The concentration of Ni bound to the AFeOx and CFeOx fractions was significantly increased by application of Si levels from S_0 to S_2 by 13.6% and 6.5%, respectively (Table 4). Belton et al. (2012) demonstrated that exogenous silicon application resulted in the attachment of silicate to the surface of iron oxide in the form of a polymer. Following the complexation of ferrosilicon, a significant number of negatively charged functional groups, including silanol, were formed. These groups provided numerous adsorption sites for PTEs, ultimately reducing their bioavailability (Belton et al., 2012). In general, all the biochars caused a significant increase in Ni content in the form of CFeOx, and there were no significant differences among the SM500, RH300 and RH500 treatments (Table 4). However, only the RH500 treatment increased the Ni concentration in the AFeOx fraction compared to control (Table 4). Among all the biochars, only the SM300 resulted in a significant increase in the Ni concentration in the Res fraction compared to the control (Table 4). The main (mean) effects of Si application showed that increasing the Si levels from S_0 to S_2 had no statistically significant effect on the Ni content in the Res fraction (Table 4).

Mailakeba and Bk (2021) studied the addition of kunai grass biochar (0.75%) to a soil with different Ni contamination levels (0, 56, 100, and 180 mg Ni kg^{-1} soil). They found that the

application of the grass biochar increased Ni content in the Res fraction and reduced Ni in the other fractions in the soil. In another study, Boostani et al. (2023c) demonstrated that the application of biochars (cow manure, municipal compost and licorice root pulp each at 3%(w/w)) to a Ni-contaminated soil increased Ni concentration in the fractions of OM and Res, and decreased Ni content in the fractions of WsEx, Car, and Fe/Mn oxide. Whereas, Boostani et al. (2023b) found that the application of manure and compost biochars (3% w/w) to Pb-contaminated soil did not significantly affect the content of Pb in the Res fraction but did decrease the WsEx fraction. Therefore, it seems that the effect of biochars on the changes of chemical fractions of PTEs in soil depends on the raw materials and production conditions of the biochar, the soil application levels, type of PTEs, the degree of soil contamination with PTEs, the selection of sequential extraction procedure and the soil properties (Mailakeba and Bk, 2021; Boostani et al., 2023b, a; Boostani et al., 2021).

In summary, the application of biochars in the present study resulted in the transfer of Ni in soil from more bioavailable and mobile fractions (WsEx, MnOx, OM) into other stable fractions (AFeOx and CFeOx). These changes were more evident in the WsEx fraction when SM biochars were applied in conjunction with Si (23-36% reduction in Ni content in the WsEx fraction compared to 13-15% when applied alone), indicating that the simultaneous application of these two substances is much more effective than applying them separately.

3.5 Ni concentration in corn (*Zea mays L.*) shoots as affected by treatments

The main effects of biochars, Si application levels and their interactive effects were statistically significant ($P < 0.01$) on the Ni concentration in corn shoots. The main (mean) effects of Si application levels showed that changing the Si levels from S_0 to S_2 resulted in 32% decrease in the Ni concentration in shoots from 8.56 mg Ni kg^{-1} dry matter (DM) to 5.82 mg Ni kg^{-1} DM (Table 5). In addition, the Ni concentration in shoots was significantly decreased by application of all the biochar treatments compared to the control (with no biochar addition) (Table 5). The interactive effects of treatments indicated that the lowest Ni concentration in shoots was observed in the combined treatment of SM500+S_2 (4.45 mg Ni kg^{-1} DM), which showed a 57.2% decrease compared to the control (CS$_0$: without Si and biochar addition) (10.4 mg Ni kg^{-1} DM) (Table 5). The Ni content in shoots had a significant and positive correlation with the Ni content in the WsEx fraction ($r = +0.62, P < 0.01$) while there were a significant and negative correlation between the soil pH ($r = -0.60, P < 0.01$) and Ni content in the CFeOx fraction ($r = -0.50, P < 0.01$) (Supplementary information). This indicates that the application of Si and biochar can reduce the Ni content in shoots by increasing soil pH and, as a result, reducing the amount of Ni in the fraction of WsEx and increasing the Ni content attached to the CFeOx fraction. Boostani et al. (2019a) reported a significant reduction in the concentration of Ni in spinach (*Spinacia oleracea* L.) shoots due to the application of rice husk and licorice root pulp biochars (2.5% w/w) in a Ni-contaminated calcareous soil. Additionally, they reported that the biochars produced at 350 °C were more effective at reducing crop Ni uptake and promoting plant growth than the biochars produced at 550 °C. The most significant factors that contribute to the uptake reduction of PTEs by plants in contaminated soils that have been amended with biochars include adsorption of heavy metals by surface functional groups , increased soil pH, reducing the mobility of PTEs by changing soil redox conditions, improved physical and biological properties of the soil, changes in the activity levels of antioxidant enzymes, and a decrease in the transfer of PTEs to the plant shoots (Zeng et al.,

2018; Rizwan et al., 2016). Several studies have investigated the effect of Si application on Ni concentration in shoots and other heavy metals in various plant species. Khaliq et al. (2016) observed a notable increase Ni concentration and accumulation within the leaf, stem, and roots of cotton after Ni application. Whereas, Si application was observed to induce a significant reduction in Ni concentrations across these respective plant components. In another study, Maryam et al. (2024) concluded that addition of Si caused an increase in the growth indices of maize through reducing the Pb concentration in shoots. One possible explanation for the reduction of Ni concentration in shoots is that Si can compete with Ni for uptake by plant roots. Silicon has a similar ionic radius to Ni, which means that it can occupy the same binding sites on root cell membranes and reduce the uptake of Ni. Additionally, Si can induce the expression of genes that are involved in Ni transport and homeostasis, which may contribute to the reduced Ni concentration in shoots (Hossain et al., 2012; Liang et al., 2005).

Table 5
Ni concentration (mg Ni kg^{-1} DM) in corn shoots as affected by biochars and Si application levels.

	C	SM300	SM500	RH300	RH500	Mean
S_0	10.4 a	7.35 bc	9.85 a	7.55 bc	7.65 b	**8.56 A**
S_1	7.65 b	6.90 bc	6.60 cd	7.05 bc	7.35 bc	**7.11 B**
S_2	7.20 bc	5.05 ef	4.45 f	5.80 de	6.60 cd	**5.82 C**
Mean	**8.41 A**	**6.43 C**	**6.96 BC**	**6.80 BC**	**7.20 B**	

Notes: C, control; SM300, sheep manure biochar generated at 300 °C; SM500, sheep manure biochar generated at 500 °C; RH300, rice husk biochar produced at 300 °C; RH500, rice husk biochar produced at 500 °C; S_0, without Si application; S_1, addition of 250 mg Si kg^{-1} soil; S_2, addition of 500 mg Si kg^{-1} soil. Numbers followed by same letters in each section, are not significantly (P<0.05) different.

3.6 Ni desorption in soil as affected by Si application levels and biochars

The cumulative Ni desorption (extracted by DTPA) in the soil as a function of time are shown in Figure 6. The release of Ni from the soil initially proceeded at a much higher rate during the first hour, and then proceeded at a much slower rate during the next 24 hours, as illustrated by the trend-line in Figure 6. This two-stage process of releasing heavy metals from soil has also been reported by other researchers (Sajadi Tabar and Jalali, 2013; Boostani et al., 2023b). It is likely that the first stage of Ni release is related to forms that are less strongly attached to soil particles, including WsEx and Car, while the second stage of Ni desorption is likely from soil chemical fractions with less bioavailability, such as FeOx and Res (Saffari et al., 2015). In general, the amount of Ni desorption in the soil was reduced by addition of biochars and Si levels (Fig. 6). In addition, the effects of biochars produced at the higher pyrolysis temperature (500 °C) on reducing Ni release was more than those generated at the lower pyrolysis temperature (300 °C) in the soil. The highest amount of Ni release was due to the control (CS$_0$: without biochar and Si application) (37.84 mg Ni kg^{-1} soil) while the lowest was observed in the combined application of SM500 and S$_2$ (31.13 mg Ni kg^{-1} soil) treatment.

498

499
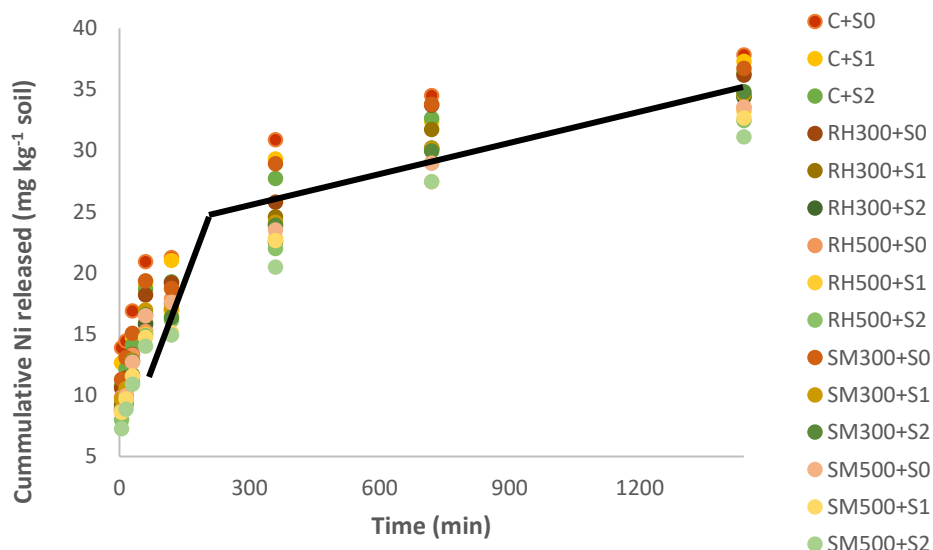
Fig. 6. Cumulative Ni desorption (extracted by DTPA) (mg kg^{-1}) in the soil as affected by different treatments. Notes: C, control; SM300, sheep manure biochar produced at 300°C; SM500, sheep manure biochar produced at 500°C; RH300, rice husk biochar produced at 300°C; RH500, rice husk biochar produced at 500°C; S$_0$, without Si addition; S$_1$, application of 250 mg Si kg^{-1} soil; S$_2$, application of 500 mg Si kg^{-1} soil.

3.7 Fitting of Ni release data to kinetic models

The Ni release data during 24 hours for all the biochar and Si treatments were evaluated by seven different kinetic models (Table 6). The effectiveness of the various kinetic models to describe the observed Ni desorption in the soil was analyzed by considering the coefficient of determination (R^2) and standard error of estimate (SEE), so that the highest value of the R^2 and the lowest value of the SEE were set as the criteria. As seen in Table 6, the order kinetic models did not adequately describe Ni release in the soil, and with the increase in the order of the kinetic model (from zero to third), the value of the R^2 decreased. This has also been found by other researchers for the release of heavy metals from soil (Boostani et al., 2019b; Ghasemi-Fasaei et al., 2006). Whereas, the non-order kinetic models, including power function, parabolic diffusion and simple Elovich, acceptably described the Ni release in the soil amended with various treatments (Table 6). Among them, the power function model was the best according to the highest value of R^2 (0.98) and the lowest value of SEE (0.055). Boostani et al. (2018a) also reported that the power function was the best kinetic model to describe Cd desorption in a Cd-contaminated soil treated with biochars and zeolite.

519

520

521

522

523

524

Table 6
The range of coefficients of determination (R^2) and standard error of estimate (SEE) of applied kinetic models to all the soil treatments.

Kinetic models	R^2		SEE	
	Range	Mean	Range	Mean
Zero order	0.79-0.87	0.80	3.36-4.67	3.67
First order	0.69-0.75	0.75	0.22-0.29	0.25
Second order	0.53-0.61	0.52	$(1.10\text{-}2.60) \times 10^{-2}$	1.80×10^{-2}
Third order	0.39-0.51	0.41	$(1.30\text{-}5.20) \times 10^{-3}$	3.00×10^{-3}
Parabolic diffusion	0.94-0.98	0.96	1.26-2.44	1.85
Power function	0.97-0.99	0.98	0.05-0.06	0.05
Simple Elovich	0.92-0.97	0.95	2.04-2.78	2.50

525

526 3.8 Using the parameters of power function model to investigate the effect of treatments on Ni
527 desorption in soil

528   As the power function model ($q = at^b$) described the Ni release data the best, its
529 parameters (a and b) were used to investigate the effect of biochar application and Si levels on the
530 release of Ni in the Ni-contaminated soil (Table 7). The main effects of biochars and Si levels and
531 their interactions on the ꞌaꞌ and ꞌbꞌ parameters were significant ($P < 0.01$). As Dang et al. (1994)
532 reported, in this kinetic model, a decrease in parameter ꞌaꞌ and an increase in parameter ꞌbꞌ indicates
533 a decrease in the rate of heavy metal desorption from the soil. The main effects of the treatments
534 showed that addition of all 4 biochars caused a significant decrease in the ꞌaꞌ parameter compared
535 to the control while the ꞌbꞌ parameter was significantly increased (Table 7). The same trend was
536 observed for all the Si treatment levels (Table 7). Therefore, it can be concluded that the use of all
537 the biochars and Si levels caused a decrease in the rate of Ni release in the Ni-contaminated soil.
538 Generally, there was a greater decrease in Ni desorption in biochar treatments prepared at the
539 higher temperature (Table 7). The interactive effects indicate that the most effective combined
540 treatment in reducing the rate of Ni release in the soil was SM500+S2 which had the lowest value
541 of parameter ꞌaꞌ (4.52) and the highest value of parameter ꞌbꞌ (0.26) among the treatments.

542   If it is differentiated from the power function equation ($q = at^b$) with respect to time (t)
543 ($dq/dt = ab\ t^{\,b\text{-}1}$), when $t = 1$ s = 0, the ratio of dq/dt becomes ꞌabꞌ. This parameter indicates the
544 amount of heavy metal desorption in the initial time (Dalal, 1985). The ꞌabꞌ parameter was affected
545 by the application of Si levels and biochars, so that this parameter was significantly decreased
546 compared to the control with addition of all the biochars (12.4%, 24.2%, 15.4% and 21.3% for the
547 SM300, SM500, RH300 and RH500, respectively) and Si application levels (13% from S_0 to S_2),
548 (Table 7). This finding also confirmed the effect of applied treatments in reducing the amount of
549 Ni release. The greatest reduction was observed in the combined treatment of SM500+S2 by 33.5%
550 compared to the control (Table 7).

551

552

553

Table 7

The coefficients of the power function model as affected by biochars and Si application levels in a Ni-polluted calcareous soil after corn cultivation.

	C	SM300	SM500	RH300	RH500	
			a (mg Ni kg^{-1} h^{-1})^b			
S_0	9.15 a	7.39 c	5.56 gh	6.49 e	5.95 f	**6.91 A**
S_1	7.92 b	6.01 f	5.23 i	5.66 g	5.21 i	**6.00 B**
S_2	6.90 d	5.39 hi	4.52 k	5.22 i	4.84 j	**5.38 C**
Mean	**7.99 A**	**6.27 B**	**5.11 E**	**5.80 C**	**5.34 D**	
			b (mg Ni kg^{-1})$^{-1}$			
S_0	0.20 g	0.22 e	0.25 b	0.24 c	0.24 c	**0.23 C**
S_1	0.21 f	0.24 c	0.25 b	0.25 b	0.25 b	**0.24 B**
S_2	0.23 d	0.25 b	0.26 a	0.26 a	0.26 a	**0.25 A**
Mean	**0.21 C**	**0.24 B**	**0.25 A**	**0.25 A**	**0.25 A**	
			ab			
S_0	1.79 a	1.68 c	1.37 h	1.54 e	1.41 g	**1.55 A**
S_1	1.69 b	1.43 f	1.29 k	1.41 fg	1.32 j	**1.42 B**
S_2	1.59 d	1.37 h	1.19 m	1.34 i	1.27 l	**1.35 C**
Mean	**1.69 A**	**1.48 B**	**1.28 E**	**1.43 C**	**1.33 D**	

Notes: C, control; SM300, sheep manure biochar produced at 300 °C; SM500, sheep manure biochar produced at 500 °C; RH300, rice husk biochar produced at 300 °C; RH500, rice husk biochar produced at 500 °C; S_0, without Si addition; S_1, application of 250 mg Si kg^{-1} soil; S_2, application of 500 mg Si kg^{-1} soil.

* Numbers followed by same letters in each column and rows, in each section, are not significantly ($P<0.05$) different

The correlation between the parameters of the fitted power function model with Ni content in various soil chemical fractions, Ni concentration in corn shoots and soil pH are shown in Table 8. The ˈaˈ and ˈabˈ parameters had a positive correlation with the Ni content in the WsEx, OM and MnOx fractions, while theses parameters had a negative correlation with the Ni content in the AFeOx and CFeOx fractions. This trend was inverse for the ˈbˈ parameter of the power function model. These correlations verified that the application of Si and biochar to the Ni-contaminated calcareous soil led to a decrease in the rate and amount of Ni release by reducing the Ni concentration in chemical forms with higher bioavailability including WsEx, OM and MnOx. Furthermore, the ˈaˈ and ˈabˈ parameters were negatively correlated with soil pH. Whereas there were positive correlations between these parameters and Ni concentration in shoots (Table 8). These findings once again confirmed that the increase in soil pH due to the application of Si and biochar can cause a decrease in bioavailability of Ni in the soil and, as a result, a decrease in the concentration of Ni in aerial parts of the plant.

Table 8

The Pearson correlation coefficients (r) among the power function model parameters (a, b, ab) with Ni content in soil chemical fractions, Ni concentration in corn shoots and soil pH.

	WsEx	Car	OM	MnOx	AFeOx	CFeOx	Res	Ni content in shoots	Soil pH
a	0.63**	0.02ns	0.70**	0.53**	-0.44**	-0.80**	0.27ns	0.62**	-0.52**
b	-0.59**	0.03ns	-0.68**	-0.54**	0.46**	0.83**	-0.28ns	-0.63**	0.51**
ab	0.68**	0.04ns	0.74**	0.46**	-0.46**	-0.80**	0.29ns	0.06**	-0.51**

Notes: WsEx, water soluble and exchangeable fraction; OM, organic fraction; MnOx, bound to manganese oxides; AFeOx, bound to amorphous iron oxides; CFeOx, bound to crystalline iron oxides; Res, residual fraction.

570

4 Conclusions

The application of biochars and Si in the present study resulted in the transfer of Ni in soil from more bioavailable and mobile fractions (WsEx, MnOx, OM) to more stable forms (AFeOx and CFeOx). These changes were particularly evident in the WsEx fraction when SM biochars were applied in conjunction with silicon, indicating a strong synergistic effect related to soil pH increase. Application of all biochars and Si reduced DPTA-extractable Ni release in the soil, which was most strongly associated with the increase in Ni content in the CFeOx fraction. Application of all the biochars and Si decreased corn Ni uptake, with the combined SM500+S_2 being the most effective. The decrease in corn uptake was correlated with the decrease in Ni content in the WsEx fraction and increase in the CFeOx fraction. SM500 was likely the most effective biochar due to its higher alkalinity and ash content, and lower acidic functional group content which enhances Ni sorption reactions with Si. Future research is needed to better understand the mechanisms underlying the interaction effects of Si and biochar application on the distribution of Ni in different soil chemical fractions and to optimize Si application strategies for sustainable Ni management in agricultural and natural ecosystems. It is suggested that the interactive effects of Si and biochar on the Ni content in soil chemical fractions and its release in aged Ni-contaminated soils should also be investigated and compared, as this study was limited to a recently Ni-contaminated soil.

588

Authors' Contributions H.R.B. Conceptualization, Formal analysis, Methodology, Investigation, Validation A.G.H. Writing - Review & Editing M.N. Project administration, Visualization E.B. Review & Editing E.F. Laboratory analyses.

Financial support. No funding was received for conducting this study.

Competing interests. The contact author has declared that neither they nor their co-authors have any competing interests.

Data availability. The data generated in this study are available from the corresponding authors upon reasonable request.

Disclaimer. Publisher's note: Copernicus Publications remains neutral with regard to jurisdictional claims in published maps and institutional affiliations.

Acknowledgements: This work was supported by College of Agriculture and Natural Resources of Darab, Shiraz University, Darab, Iran.

References

Abdelhafez, A. A., Li, J., and Abbas, M. H.: Feasibility of biochar manufactured from organic wastes on the stabilization of heavy metals in a metal smelter contaminated soil, Chemosphere, 117, 66-71, 2014.

Adrees, M., Ali, S., Rizwan, M., Zia-ur-Rehman, M., Ibrahim, M., Abbas, F., Farid, M., Qayyum, M. F., and Irshad, M. K.: Mechanisms of silicon-mediated alleviation of heavy metal toxicity in plants: a review, Ecotoxicology and Environmental Safety, 119, 186-197, 2015.

Ahmad, M., Rajapaksha, A. U., Lim, J. E., Zhang, M., Bolan, N., Mohan, D., Vithanage, M., Lee, S. S., and Ok, Y. S.: Biochar as a sorbent for contaminant management in soil and water: a review, Chemosphere, 99, 19-33, 2014.

Alam, M. S., Gorman-Lewis, D., Chen, N., Flynn, S. L., Ok, Y. S., Konhauser, K. O., and Alessi, D. S.: Thermodynamic analysis of nickel (II) and zinc (II) adsorption to biochar, Environmental science & technology, 52, 6246-6255, 2018.

Anand, A., Gautam, S., and Ram, L. C.: Feedstock and pyrolysis conditions affect suitability of biochar for various sustainable energy and environmental applications, Journal of Analytical and Applied Pyrolysis, 170, 105881, 2023.

Ankita Rao, K., Nair, V., Divyashri, G., Krishna Murthy, T., Dey, P., Samrat, K., Chandraprabha, M., and Hari Krishna, R.: Role of Lignocellulosic Waste in Biochar Production for Adsorptive Removal of Pollutants from Wastewater, in: Advanced and Innovative Approaches of Environmental Biotechnology in Industrial Wastewater Treatment, Springer, 221-238, 2023.

Antoniadis, V., Levizou, E., Shaheen, S. M., Ok, Y. S., Sebastian, A., Baum, C., Prasad, M. N., Wenzel, W. W., and Rinklebe, J.: Trace elements in the soil-plant interface: Phytoavailability, translocation, and phytoremediation–A review, Earth-Science Reviews, 171, 621-645, 2017.

Bandara, T., Franks, A., Xu, J., Bolan, N., Wang, H., and Tang, C.: Chemical and biological immobilization mechanisms of potentially toxic elements in biochar-amended soils, Critical Reviews in Environmental Science and Technology, 50, 903-978, 2020.

Belton, D. J., Deschaume, O., and Perry, C. C.: An overview of the fundamentals of the chemistry of silica with relevance to biosilicification and technological advances, The FEBS journal, 279, 1710-1720, 2012.

Bharti, K. P., Pradhan, A. K., Singh, M., Beura, K., Behera, S. K., and Paul, S. C.: Effect of mycorrhizal co-Inoculation with selected rhizobacteria on soil zinc dynamics, International Journal of Current Microbiology and Applied Sciences, 7, 1961-1970, 2018.

Bhat, J. A., Shivaraj, S., Singh, P., Navadagi, D. B., Tripathi, D. K., Dash, P. K., Solanke, A. U., Sonah, H., and Deshmukh, R.: Role of silicon in mitigation of heavy metal stresses in crop plants, Plants, 8, 71, 2019.

Boostani, H., Hardie, A., Najafi-Ghiri, M., and Khalili, D.: Investigation of cadmium immobilization in a contaminated calcareous soil as influenced by biochars and natural zeolite application, International Journal of Environmental Science and Technology, 15, 2433-2446, 2018a.

Boostani, H., Hardie, A., Najafi-Ghiri, M., and Khalili, D.: Investigation of cadmium immobilization in a contaminated calcareous soil as influenced by biochars and natural zeolite application, International journal of environmental science and technology, 15, 2433-2446, 2018b.

Boostani, H. R., HARDIE, A. G., and NAJAFI-GHIRI, M.: Lead stabilization in a polluted calcareous soil using cost-effective biochar and zeolite amendments after spinach cultivation, Pedosphere, 33, 321-330, 2023a.

Boostani, H. R., Hardie, A. G., and Najafi-Ghiri, M.: Chemical fractions, mobility and release kinetics of Cadmium in a light-textured calcareous soil as affected by crop residue biochars and Cd-contamination levels, Chemistry and Ecology, 1-14, 2023b.

Boostani, H. R., Najafi-Ghiri, M., and Mirsoleimani, A.: The effect of biochars application on reducing the toxic effects of nickel and growth indices of spinach (Spinacia oleracea L.) in a calcareous soil, Environmental Science and Pollution Research, 26, 1751-1760, 2019a.

Boostani, H. R., Hardie, A. G., Najafi-Ghiri, M., and Khalili, D.: The effect of soil moisture regime and biochar application on lead (Pb) stabilization in a contaminated soil, Ecotoxicology and Environmental Safety, 208, 111626, 2021.

Boostani, H. R., Hardie, A. G., Najafi-Ghiri, M., and Zare, M.: Chemical speciation and release kinetics of Ni in a Ni-contaminated calcareous soil as affected by organic waste biochars and soil moisture regime, Environmental Geochemistry and Health, 45, 199-213, 2023c.

657 Boostani, H. R., Najafi-Ghiri, M., Amin, H., and Mirsoleimani, A.: Zinc desorption kinetics from some
658   calcareous soils of orange (Citrus sinensis L.) orchards, southern Iran, Soil science and plant
659   nutrition, 65, 20-27, 2019b.
660 Chatterjee, R., Sajjadi, B., Chen, W.-Y., Mattern, D. L., Hammer, N., Raman, V., and Dorris, A.: Effect
661   of pyrolysis temperature on physicochemical properties and acoustic-based amination of biochar
662   for efficient CO2 adsorption, Frontiers in Energy Research, 8, 85, 2020.
663 Claoston, N., Samsuri, A., Ahmad Husni, M., and Mohd Amran, M.: Effects of pyrolysis temperature on
664   the physicochemical properties of empty fruit bunch and rice husk biochars, Waste Management
665   & Research, 32, 331-339, 2014.
666 Dalal, R.: Comparative prediction of yield response and phosphorus uptake from soil using anion-and
667   cation-anion-exchange resins, Soil Science, 139, 227-231, 1985.
668 Dang, Y., Dalal, R., Edwards, D., and Tiller, K.: Kinetics of zinc desorption from Vertisols, Soil Science
669   Society of America Journal, 58, 1392-1399, 1994.
670 Deng, Y., Huang, S., Laird, D. A., Wang, X., and Meng, Z.: Adsorption behaviour and mechanisms of
671   cadmium and nickel on rice straw biochars in single-and binary-metal systems, Chemosphere,
672   218, 308-318, 2019.
673 Derakhshan Nejad, Z., Jung, M. C., and Kim, K.-H.: Remediation of soils contaminated with heavy
674   metals with an emphasis on immobilization technology, Environmental geochemistry and health,
675   40, 927-953, 2018.
676 Dey, D., Sarangi, D., and Mondal, P.: Biochar: Porous Carbon Material, Its Role to Maintain Sustainable
677   Environment, in: Handbook of Porous Carbon Materials, Springer, 595-621, 2023.
678 El-Naggar, A., Rajapaksha, A. U., Shaheen, S. M., Rinklebe, J., and Ok, Y. S.: Potential of biochar to
679   immobilize nickel in contaminated soils, in: Nickel in Soils and Plants, CRC Press, 293-318,
680   2018.
681 El-Naggar, A., Chang, S. X., Cai, Y., Lee, Y. H., Wang, J., Wang, S.-L., Ryu, C., Rinklebe, J., and Ok, Y.
682   S.: Mechanistic insights into the (im) mobilization of arsenic, cadmium, lead, and zinc in a multi-
683   contaminated soil treated with different biochars, Environment International, 156, 106638, 2021.
684 Gao, W., He, W., Zhang, J., Chen, Y., Zhang, Z., Yang, Y., and He, Z.: Effects of biochar-based materials
685   on nickel adsorption and bioavailability in soil, Scientific Reports, 13, 5880, 2023.
686 Gee, G. W. and Bauder, J. W.: Particle-size analysis, Methods of soil analysis: Part 1 Physical and
687   mineralogical methods, 5, 383-411, 1986.
688 Ghasemi-Fasaei, R., Maftoun, M., Ronaghi, A., Karimian, N., Yasrebi, J., Assad, M., and Ippolito, J.:
689   Kinetics of copper desorption from highly calcareous soils, Communications in Soil Science and
690   Plant Analysis, 37, 797-809, 2006.
691 Ghiri, M. N., Abtahi, A., Owliaie, H., Hashemi, S. S., and Koohkan, H.: Factors affecting potassium
692   pools distribution in calcareous soils of southern Iran, Arid land research and management, 25,
693   313-327, 2011.
694 Hossain, M. A., Piyatida, P., da Silva, J. A. T., and Fujita, M.: Molecular mechanism of heavy metal
695   toxicity and tolerance in plants: central role of glutathione in detoxification of reactive oxygen
696   species and methylglyoxal and in heavy metal chelation, Journal of botany, 2012, 2012.
697 Ippolito, J., Berry, C., Strawn, D., Novak, J., Levine, J., and Harley, A.: Biochars reduce mine land soil
698   bioavailable metals, Journal of environmental quality, 46, 411-419, 2017.
699 Jalali, M., Beygi, M., Jalali, M., and Buss, W.: Background levels of DTPA-extractable trace elements in
700   calcareous soils and prediction of trace element availability based on common soil properties,
701   Journal of Geochemical Exploration, 241, 107073, 2022.
702 Kamali, S., Ronaghi, A., and Karimian, N.: Soil zinc transformations as affected by applied zinc and
703   organic materials, Communications in soil science and plant analysis, 42, 1038-1049, 2011.
704 Kameyama, K., Miyamoto, T., and Iwata, Y.: The preliminary study of water-retention related properties
705   of biochar produced from various feedstock at different pyrolysis temperatures, Materials, 12,
706   1732, 2019.

Kandpal, G., Srivastava, P., and Ram, B.: Kinetics of desorption of heavy metals from polluted soils: Influence of soil type and metal source, Water, Air, and Soil Pollution, 161, 353-363, 2005.

Keiluweit, M., Nico, P. S., Johnson, M. G., and Kleber, M.: Dynamic molecular structure of plant biomass-derived black carbon (biochar), Environmental science & technology, 44, 1247-1253, 2010.

Khaliq, A., Ali, S., Hameed, A., Farooq, M. A., Farid, M., Shakoor, M. B., Mahmood, K., Ishaque, W., and Rizwan, M.: Silicon alleviates nickel toxicity in cotton seedlings through enhancing growth, photosynthesis, and suppressing Ni uptake and oxidative stress, Archives of Agronomy and Soil Science, 62, 633-647, 2016.

Li, X.: Technical solutions for the safe utilization of heavy metal-contaminated farmland in China: a critical review, Land Degradation & Development, 30, 1773-1784, 2019.

Liang, Y., Wong, J., and Wei, L.: Silicon-mediated enhancement of cadmium tolerance in maize (Zea mays L.) grown in cadmium contaminated soil, Chemosphere, 58, 475-483, 2005.

Lindsay, W. L. and Norvell, W.: Development of a DTPA soil test for zinc, iron, manganese, and copper, Soil science society of America journal, 42, 421-428, 1978.

Liu, L., Guo, X., Wang, S., Li, L., Zeng, Y., and Liu, G.: Effects of wood vinegar on properties and mechanism of heavy metal competitive adsorption on secondary fermentation based composts, Ecotoxicology and environmental safety, 150, 270-279, 2018.

Loeppert, R. H. and Suarez, D. L.: Carbonate and gypsum, Methods of soil analysis: Part 3 chemical methods, 5, 437-474, 1996.

Lu, K., Yang, X., Gielen, G., Bolan, N., Ok, Y. S., Niazi, N. K., Xu, S., Yuan, G., Chen, X., and Zhang, X.: Effect of bamboo and rice straw biochars on the mobility and redistribution of heavy metals (Cd, Cu, Pb and Zn) in contaminated soil, Journal of environmental management, 186, 285-292, 2017.

Ma, C., Ci, K., Zhu, J., Sun, Z., Liu, Z., Li, X., Zhu, Y., Tang, C., Wang, P., and Liu, Z.: Impacts of exogenous mineral silicon on cadmium migration and transformation in the soil-rice system and on soil health, Science of the Total Environment, 759, 143501, 2021.

Mailakeba, C. D. and BK, R. R.: Biochar application alters soil Ni fractions and phytotoxicity of Ni to pakchoi (Brassica rapa L. ssp. chinensis L.) plants, Environmental Technology & Innovation, 23, 101751, 2021.

Maruyama, M., Sawada, K. P., Tanaka, Y., Okada, A., Momma, K., Nakamura, M., Mori, R., Furukawa, Y., Sugiura, Y., and Tajiri, R.: Quantitative analysis of calcium oxalate monohydrate and dihydrate for elucidating the formation mechanism of calcium oxalate kidney stones, Plos one, 18, e0282743, 2023.

Maryam, H., Abbasi, G. H., Waseem, M., Ahmed, T., and Rizwan, M.: Preparation and characterization of green silicon nanoparticles and their effects on growth and lead (Pb) accumulation in maize (Zea mays L.), Environmental Pollution, 123691, 2024.

Myszka, B., Schüßler, M., Hurle, K., Demmert, B., Detsch, R., Boccaccini, A. R., and Wolf, S. E.: Phase-specific bioactivity and altered Ostwald ripening pathways of calcium carbonate polymorphs in simulated body fluid, RSC advances, 9, 18232-18244, 2019.

Nasrabadi, M., Omid, M. H., and Mazdeh, A. M.: Experimental Study of Flow Turbulence Effect on Cadmium Desorption Kinetics from Riverbed Sands, Environmental Processes, 9, 10, 2022.

Nelson, D. W. and Sommers, L. E.: Total carbon, organic carbon, and organic matter, Methods of soil analysis: Part 3 Chemical methods, 5, 961-1010, 1996.

Poznanović Spahić, M. M., Sakan, S. M., Glavaš-Trbić, B. M., Tančić, P. I., Škrivanj, S. B., Kovačević, J. R., and Manojlović, D. D.: Natural and anthropogenic sources of chromium, nickel and cobalt in soils impacted by agricultural and industrial activity (Vojvodina, Serbia), Journal of Environmental Science and Health, Part A, 54, 219-230, 2019.

Rassaei, F., Hoodaji, M., and Abtahi, S. A.: Fractionation and mobility of cadmium and zinc in calcareous soils of Fars Province, Iran, Arabian Journal of Geosciences, 13, 1-7, 2020.

757 Rhoades, J.: Salinity: Electrical conductivity and total dissolved solids, Methods of soil analysis: Part 3
758   Chemical methods, 5, 417-435, 1996.
759 Rizwan, M., Ali, S., Qayyum, M. F., Ibrahim, M., Zia-ur-Rehman, M., Abbas, T., and Ok, Y. S.:
760   Mechanisms of biochar-mediated alleviation of toxicity of trace elements in plants: a critical
761   review, Environmental Science and Pollution Research, 23, 2230-2248, 2016.
762 Sachdeva, S., Kumar, R., Sahoo, P. K., and Nadda, A. K.: Recent advances in biochar amendments for
763   immobilization of heavy metals in an agricultural ecosystem: A systematic review,
764   Environmental Pollution, 319, 120937, 2023.
765 Saffari, M., Karimian, N., Ronaghi, A., Yasrebi, J., and Ghasemi-Fasaei, R.: Stabilization of nickel in a
766   contaminated calcareous soil amended with low-cost amendments, Journal of soil science and
767   plant nutrition, 15, 896-913, 2015.
768 Sajadi Tabar, S. and Jalali, M.: Kinetics of Cd release from some contaminated calcareous soils, Natural
769   resources research, 22, 37-44, 2013.
770 Shahbazi, K., Fathi-Gerdelidani, A., and Marzi, M.: Investigation of the status of heavy metals in soils of
771   Iran: A comprehensive and critical review of reported studies, Iranian Journal of Soil and Water
772   Research, 53, 1163-1212, 10.22059/ijswr.2022.341586.669245, 2022.
773 Shahbazi, K., Marzi, M., and Rezaei, H.: Heavy metal concentration in the agricultural soils under the
774   different climatic regions: a case study of Iran, Environmental earth sciences, 79, 324, 2020.
775 Shahzad, B., Tanveer, M., Rehman, A., Cheema, S. A., Fahad, S., Rehman, S., and Sharma, A.: Nickel;
776   whether toxic or essential for plants and environment-A review, Plant Physiology and
777   Biochemistry, 132, 641-651, 2018.
778 Shen, B., Wang, X., Zhang, Y., Zhang, M., Wang, K., Xie, P., and Ji, H.: The optimum pH and Eh for
779   simultaneously minimizing bioavailable cadmium and arsenic contents in soils under the organic
780   fertilizer application, Science of the Total Environment, 711, 135229, 2020.
781 Singh, J., Karwasra, S., and Singh, M.: Distribution and forms of copper, iron, manganese, and zinc in
782   calcareous soils of India, Soil Science, 146, 359-366, 1988.
783 Sparks, D. L., Singh, B., and Siebecker, M. G.: Environmental soil chemistry, Elsevier2022.
784 Sparrow, L. and Uren, N.: Manganese oxidation and reduction in soils: effects of temperature, water
785   potential, pH and their interactions, Soil Research, 52, 483-494, 2014.
786 Sumner, M. E. and Miller, W. P.: Cation exchange capacity and exchange coefficients, Methods of soil
787   analysis: Part 3 Chemical methods, 5, 1201-1229, 1996.
788 Sun, L., Zhang, G., Li, X., Zhang, X., Hang, W., Tang, M., and Gao, Y.: Effects of biochar on the
789   transformation of cadmium fractions in alkaline soil, Heliyon, e12949, 2023.
790 Sun, Y., Gao, B., Yao, Y., Fang, J., Zhang, M., Zhou, Y., Chen, H., and Yang, L.: Effects of feedstock
791   type, production method, and pyrolysis temperature on biochar and hydrochar properties,
792   Chemical engineering journal, 240, 574-578, 2014.
793 Tomczyk, A., Sokołowska, Z., and Boguta, P.: Biochar physicochemical properties: pyrolysis temperature
794   and feedstock kind effects, Reviews in Environmental Science and Bio/Technology, 19, 191-215,
795   2020.
796 Uchimiya, M., Lima, I. M., Thomas Klasson, K., Chang, S., Wartelle, L. H., and Rodgers, J. E.:
797   Immobilization of heavy metal ions (CuII, CdII, NiII, and PbII) by broiler litter-derived biochars
798   in water and soil, Journal of agricultural and food chemistry, 58, 5538-5544, 2010.
799 Vickers, N. J.: Animal communication: when i'm calling you, will you answer too?, Current biology, 27,
800   R713-R715, 2017.
801 Xiao, Z., Peng, M., Mei, Y., Tan, L., and Liang, Y.: Effect of organosilicone and mineral silicon
802   fertilizers on chemical forms of cadmium and lead in soil and their accumulation in rice,
803   Environmental Pollution, 283, 117107, 2021.
804 Yan, G.-c., Nikolic, M., YE, M.-j., Xiao, Z.-x., and LIANG, Y.-c.: Silicon acquisition and accumulation
805   in plant and its significance for agriculture, Journal of Integrative Agriculture, 17, 2138-2150,
806   2018.

807 Yuan, J.-H., Xu, R.-K., and Zhang, H.: The forms of alkalis in the biochar produced from crop residues at
808   different temperatures, Bioresource technology, 102, 3488-3497, 2011.
809 Zemnukhova, L. A., Panasenko, A. E., Artem'yanov, A. P., and Tsoy, E. A.: Dependence of porosity of
810   amorphous silicon dioxide prepared from rice straw on plant variety, BioResources, 10, 3713-
811   3723, 2015.
812 Zeng, X., Xiao, Z., Zhang, G., Wang, A., Li, Z., Liu, Y., Wang, H., Zeng, Q., Liang, Y., and Zou, D.:
813   Speciation and bioavailability of heavy metals in pyrolytic biochar of swine and goat manures,
814   Journal of Analytical and Applied Pyrolysis, 132, 82-93, 2018.
815 Zhao, S.-X., Ta, N., and Wang, X.-D.: Effect of temperature on the structural and physicochemical
816   properties of biochar with apple tree branches as feedstock material, Energies, 10, 1293, 2017.
817 Zhu, Q., Wu, J., Wang, L., Yang, G., and Zhang, X.: Effect of biochar on heavy metal speciation of paddy
818   soil, Water, Air, & Soil Pollution, 226, 1-10, 2015.
819